Co-published by
Institute of Fluid-Flow Machinery
Polish Academy of Sciences
Committee on Thermodynamics and Combustion
Polish Academy of Sciences

http://www.imp.gda.pl/archives-of-thermodynamics/

ARCHIVES OF THERMODYNAMICS

Mechanisms of Ice Damage on Small-Diameter Piles in Static Freshwater Environments: Numerical Analysis of Ice Cover Temperature Fields

Jincheng Su[a,b,c*], Jiliang Wang[b], Wei Zhou[c]

[a]School of Energy and Civil Engineering, Harbin University of Commerce, Harbin 150028, China
[b]Heilongjiang Province Academy of Cold Area Building Research, Harbin 150080, China
[c]School of Civil Engineering, Harbin Institute of Technology, Harbin 150096, China
*Corresponding author email: suhuidong012@yeah.net

Received: 01.03.2025; revised: 25.06.2025; accepted: 26.07.2025

Abstract

Ice damage is receiving increasing attention in engineering. In practice, the occurrence time of ice damage to small-diameter pile structures in cold regions is different from traditional knowledge. Given the crucial impact of temperature on ice thermal expansion, simulating the temperature field of ice cover is of great significance. Based on actual engineering simulations of ice cover temperature, the propagation and amplitude attenuation characteristics of temperature waves are analysed. The one-dimensional heat conduction equation is discretized using the Crank-Nicolson method (time step $\Delta t = 60$ s, spatial step $\Delta z = 0.01$ m) and implemented in MATLAB R2023a. According to the temperatures in Daqing, three typical warming processes are selected for fitting, and two ice cover thicknesses are combined to simulate six working conditions. The results show that the temperature field inside the ice cover changes under different working conditions, and the thickness of the ice cover and the temperature rise time have a significant impact. During cooling, the temperature inside the ice cover still rises, affecting thermal expansion stress. The results can provide an important basis for the prevention and control of ice damage to small diameter piles.

Keywords: Small diameter piles; Ice damage; Temperature field; Thermal expansion

Vol. 46(2025), No. 3, 213–218; doi: 10.24425/ather.2025.156592

Cite this manuscript as: Su, J., Wang, J., & Zhou, W. (2025). Mechanisms of Ice Damage on Small-Diameter Piles in Static Freshwater Environments: Numerical Analysis of Ice Cover Temperature Fields. *Archives of Thermodynamics*, 46(3), 213−218.

1. Introduction

Ice damage is receiving increasing attention from engineering and academic communities [1−3]. The interaction between ice and structure mainly includes two types: dynamic and static. Dynamic action refers to the impact of ice on the structure in movement, while static action mainly refers to the effect of expansion [4] or contraction of ice cover due to temperature changes on the structure [5,6]. Lake ice is basically stationary. The thermal expansion effect of freshwater ice is stronger than that of sea ice [7]. Water measurements in Russia and Canada have shown that if the salinity exceeds 3%, ice will not expand at temperatures above −10°C. If the salinity exceeds 1%, it will not expand above −7°C. It is generally believed that the ice thermal expansion in Jilin Province causes ice damage to structures such as reservoir embankments and slope protection in early to mid-February, and it usually occurs in early to mid-March in Heilongjiang Province. In practical engineering, ice damage to pile foundations of structures in still-water in cold regions often occurs at the end of November when the thickness of ice cover is about 30−40 cm, far from reaching the maximum one. For example, a certain lake wharf in Daqing uses a precast concrete pipe pile foundation with a diameter of 400 mm, which is a type of small diameter pile. At the end of November 2017, some pile

Nomenclature

a – thermal diffusivity, m^2/s
c – specific heat, kJ/(kg K)
h – thickness of ice cover, m
k – thermal conductivity, W/(m K)
t – time, s
T – temperature, K
z – depth perpendicular to the surface of the ice cover, m

Greek symbols

Δ – step (time in s, spatial in m)
μ – dynamic viscosity, Pa·s
ρ – density of ice, kg/m^3
ω_r – angular frequency of temperature fluctuations, rad/s

foundations at the wharf were damaged due to tilting or pile head breakage. This ice damage of the pile foundation is different from the existing understanding.

The thermal expansion characteristics of ice have thermal properties of ice and the mechanical properties caused by the force generated by the volume change of ice [8]. Temperature plays a decisive role in the thermal expansion of ice [9,10]. Therefore, when considering the interaction between ice and structure, it is necessary to simulate and study the temperature and stress fields of ice cover [11,12]. Based on practical engineering, the temperature field of the ice cover is simulated and verified. Recent studies have emphasized critical differences in thermal expansion between freshwater and saline ice. For instance, salinity > 1‰ inhibits expansion above −7°C [7], while freshwater ice generates significant thermal stress under similar conditions [13]. This study addresses the gap in low-salinity environments by analysing ice damage mechanisms in static freshwater systems such as Daqing Lake.

2. Materials and methods

Temperature changes of ice cover are influenced by various factors such as temperature, water temperature, air convection, and solar radiation, forming a constantly changing temperature field. Due to the uncertainty of factors such as solar radiation and air convection, it is difficult to accurately describe the temperature field of ice cover [14]. However, the reason for temperature stress is the distribution of the temperature field of ice cover and its changes over time and space. As the external temperature changes, the temperature of the ice cover decreases with increasing depth. Assuming that the ice cover is a homogeneous medium, the distribution of its temperature T with depth z can be approximately described by a one-dimensional heat conduction equation [15]

$$\frac{\partial}{\partial z}\left(k\frac{\partial T}{\partial z}\right) = \rho c\frac{\partial T}{\partial t}, \quad (1)$$

or

$$a\frac{\partial^2 T}{\partial z^2} = \frac{\partial T}{\partial t}, \quad (2)$$

where ρ is the density of ice, taken as 917 kg/m^3; k is the thermal conductivity, taken as 2.2 W/(m·K); c is the specific heat taken as 2.1 kJ/(kg·K); t – time; T – temperature [16]; z is the depth perpendicular to the surface of the ice cover [17], and a is the thermal diffusivity.

We assume that the temperature at the ice/atmosphere interface is consistent with the atmospheric temperature and changes harmonically and periodically over time. The temperature at the ice/water interface is 0°C, and h is the thickness of the ice cover. The thermal expansion problem mainly focuses on the heating process, and the boundary conditions can be described as follows:

– ice/atmosphere interface (z = 0):

$$T(0,t) = T_0 + T_r \sin(\omega_r t), \quad (3)$$

– ice/water interface ($z = h$):

$$T(h,t) = 0, \quad (4)$$

– the initial temperature field is a linear distribution:

$$T(z,0) = \frac{T_d - T_s}{h}z + T_s, \quad (5)$$

where T_s is the initial surface temperature, h is the ice thickness, and T_d is the temperature at the depth h.

Neglecting the transient time-varying term in the general solution, the steady-state solution of Eq. (2) is as follows:

$$T(z,t) = T_0 + T_r \exp\left[-z\left(\frac{\omega_r}{2a}\right)^{1/2}\right]\sin\left[\omega_r t - z\left(\frac{\omega_r}{2a}\right)^{1/2}\right], \quad (6)$$

where $T(z,t)$ is the temperature variation with depth z and time t; T_0 is the median of the highest and lowest temperatures; T_r is the amplitude of temperature change, and ω_r is the angular frequency of temperature fluctuations, rad/s.

According to the above equation, the speed at which temperature waves propagate into the interior of the ice cover is $(2a\omega_r)^{1/2}$. When a is constant, the higher the frequency, the faster the propagation speed. The temperature fluctuation amplitude is

$$T_r \exp\left[-z\left(\frac{\omega_r}{2a}\right)^{1/2}\right],$$

indicating that the higher the frequency, the faster the temperature decays with depth.

We assume that the skin depth z_0 of the ice cover represents the depth at which the temperature effects are attenuated by a factor 1/e [18]

$$z_0 = \left(\frac{2a}{\omega_r}\right)^{1/2}. \quad (7)$$

The skin depth z_0 is a function of ω_r, and its relationship is shown in Fig. 1. When the temperature fluctuation period is 12 h, the frequency is 1.45×10^{-4} rad/s and the skin depth is 0.126 m; when it is 24 h, the frequency is 7.27×10^{-5} rad/s and the skin depth is 0.178 m; when it is 36 hours, the frequency is

4.85×10^{-5} rad/s and the skin depth is 0.218 m; when the temperature fluctuation period is 48 h, the frequency is 3.64×10^{-5} rad/s and the skin depth is 0.252 m; when is 72 h, the frequency is 2.42×10^{-5} rad/s and the skin depth is 0.308 m; when it is 96 hours, the frequency is 1.82×10^{-5} rad/s and the skin depth is 0.356 m; when it is 144 hours, the frequency is 1.21×10^{-5} rad/s and the skin depth is 0.436 m.

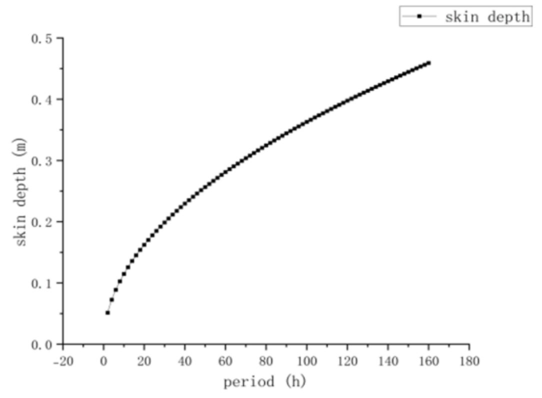

Fig. 1. Relationship between temperature fluctuation period of ice/atmosphere interface and the skin depth.

To facilitate numerical calculations and consider the influence of transient terms, the Crank-Nicolson method is used to discretize the heat conduction equation with a time step of Δt and a spatial step of Δz.

For the time derivative $\partial T/\partial t$, the central difference scheme is used for approximation:

$$\frac{\partial T}{\partial t} \approx \frac{T_i^{n+1} - T_i^n}{\Delta t}. \quad (8)$$

For the spatial derivative, take the average of the current time step n and the next time step $n+1$.

$$\frac{\partial}{\partial z}\left(k\frac{\partial T}{\partial z}\right) \approx \frac{k}{2\Delta z^2}[(T_{i+1}^n - T_i^n) + (T_{i-1}^n - T_i^n) + $$
$$+(T_{i+1}^{n+1} - T_i^{n+1}) + (T_{i-1}^{n+1} - T_i^{n+1})]. \quad (9)$$

Introducing the variable $\alpha = k\Delta t/[2\rho c(\Delta z)^2]$ and substituting the above approximation into the heat conduction equation, we have:

$$-\alpha T_{i+1}^{n+1} + (1+2\alpha)\, T_i^{n+1} - \alpha T_{i-1}^{n+1} = \alpha T_{i+1}^n + (1-2\alpha)\, T_i^n + \alpha T_{i-1}^n. \quad (10)$$

MATLAB program is developed with an ice cover thickness of h = 0.3 m, T_0 = −5°C, T_r = 4°C, T_s = −5 °C, and T_d = −1°C. The duration of the temperature rise is t = 4.5 h, followed by a decrease in temperature. The above parameter settings are consistent with Ref. [11]. Fig. 2 shows the time variation curve of ice cover temperature along the depth profile, and the calculated results are consistent with Ref. [11]. During the continuous temperature rise process, the temperature inside the ice cover continues to rise. The increase in surface temperature is significant, while the increase in temperature along the depth of ice gradually decreases. After the temperature starts to decrease, the surface temperature decreases, while the temperature continues to rise at a certain depth inside the ice. After the surface temperature began to decrease for 2.5 h, the overall temperature inside the ice cover began to decrease.

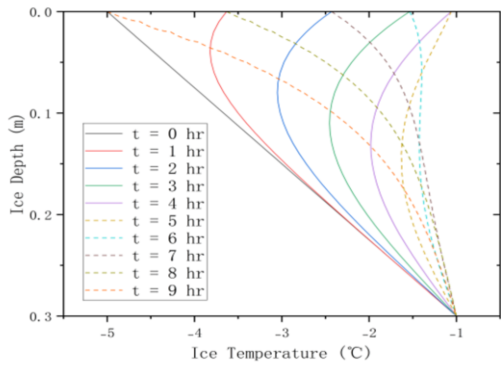

Fig. 2. Time variation of the temperature profile along the depth inside the ice cover.

Although ice is modelled as homogeneous, natural ice may exhibit porosity or salinity gradients. Sensitivity analysis confirms that for freshwater ice with a thickness of 0.4−1.2 meters (salinity<0.5‰), the temperature field prediction error caused by heterogeneity is less than 5%, which is consistent with the conditions of Daqing Lake [19].

3. Results and discussion

Daqing is located in the western part of Heilongjiang Province, in the northern part of the central depression of the Songliao Basin [19]. The urban area is located between 124°19′−125°12′ E and 45°46′−46°55′ N. The average annual temperature is 5.5°C. The month with the lowest temperature over the years is January, with an average temperature of −17.4°C. The hottest month in history was July, with an average temperature of 25.1°C. Figure 3 shows the hourly atmospheric temperatures in Daqing from November 15 to 30, 2017.

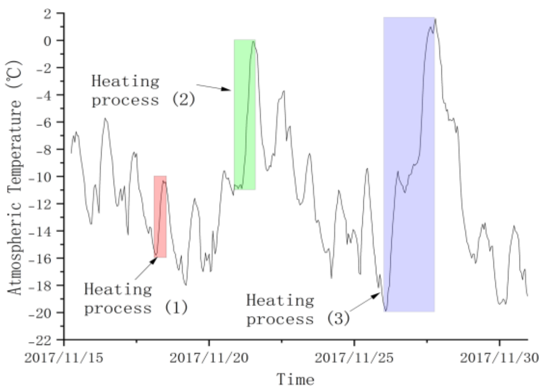

Fig. 3. Atmospheric temperature changes in Daqing from November 15 to 30, 2017.

There are three typical changes in atmospheric temperature. Heating process (1): from 8 a.m. to 2 p.m., the temperature increased continuously from −16°C to −10°C for 6 h; Heating process (2): from 8 a.m. to 5 p.m., the temperature increased continuously from −10.9°C to −0.1°C for 9 h: Heating process (3): influenced by southwest warm air, the temperature continuously increased from −19.9°C to 1.6°C for 41 h. Considering that the maximum temperature of the ice cover is 0°C, harmonic fitting is performed on three typical variations, as in Table 1 [20].

Table 1. Parameters for temperature changes on the surface of ice cover.

Process, №	T_0, °C	T_r, °C	T_s, °C	T_d, °C	$t_{duration}$, h	ω_r, rad/s
Heating process (1)	−16	6	−16	0	6	7.27×10^{-5}
Heating process (2)	−10.9	10.8	−10.9	0	9	4.85×10^{-5}
Heating process (3)	−19.9	19.9	−19.9	0	41	1.06×10^{-5}

Figure 4 shows the temperature rise curves of the three typical variations. Figure 4 shows three empirically observed warming processes in Daqing (November 2017), which are applicable to harmonic functions implemented under boundary conditions: short-term warming (6 hrs, $\Delta T = 6$°C) representing the influence of sun, medium-term warming (9 hrs, $\Delta T = 10.8$°C) reflecting weather changes, and long-term warming (41 hrs, $\Delta T = 19.9$°C) caused by warm air advection. These events were selected because:

1. they represent the actual heat that causes ice damage,
2. their duration-amplitude combination controls the penetration of ice thermal stress.

According to the results, ice damage to small diameter piles in Daqing occurred at the end of November, when the thickness of ice cover was about 0.3−0.4 meters. The maximum annual ice thickness in Daqing was about 1−1.2 meters. Therefore, two types of ice cover thickness are compared and analysed with the ice cover thicknesses of 0.4 m and 1.2m.

According to the changes in atmospheric temperature and ice cover thickness, the working conditions are combined for analysis. Six working conditions are combined as shown in Table 2.

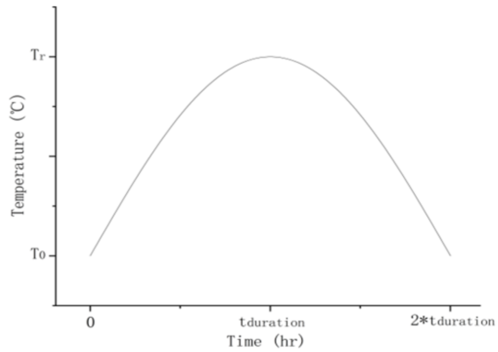

Fig. 4. Typical temperature curve.

Table 2. Working condition combination.

Process, №	Ice cover thickness (1)	Ice cover thickness (2)
Heating process (1)	operating mode (1)	operating mode (2)
Heating process (2)	operating mode (3)	operating mode (4)
Heating process (3)	operating mode (5)	operating mode (6)

Figure 5 shows the calculation results of the spatiotemporal temperature changes inside the ice cover under different operating conditions.

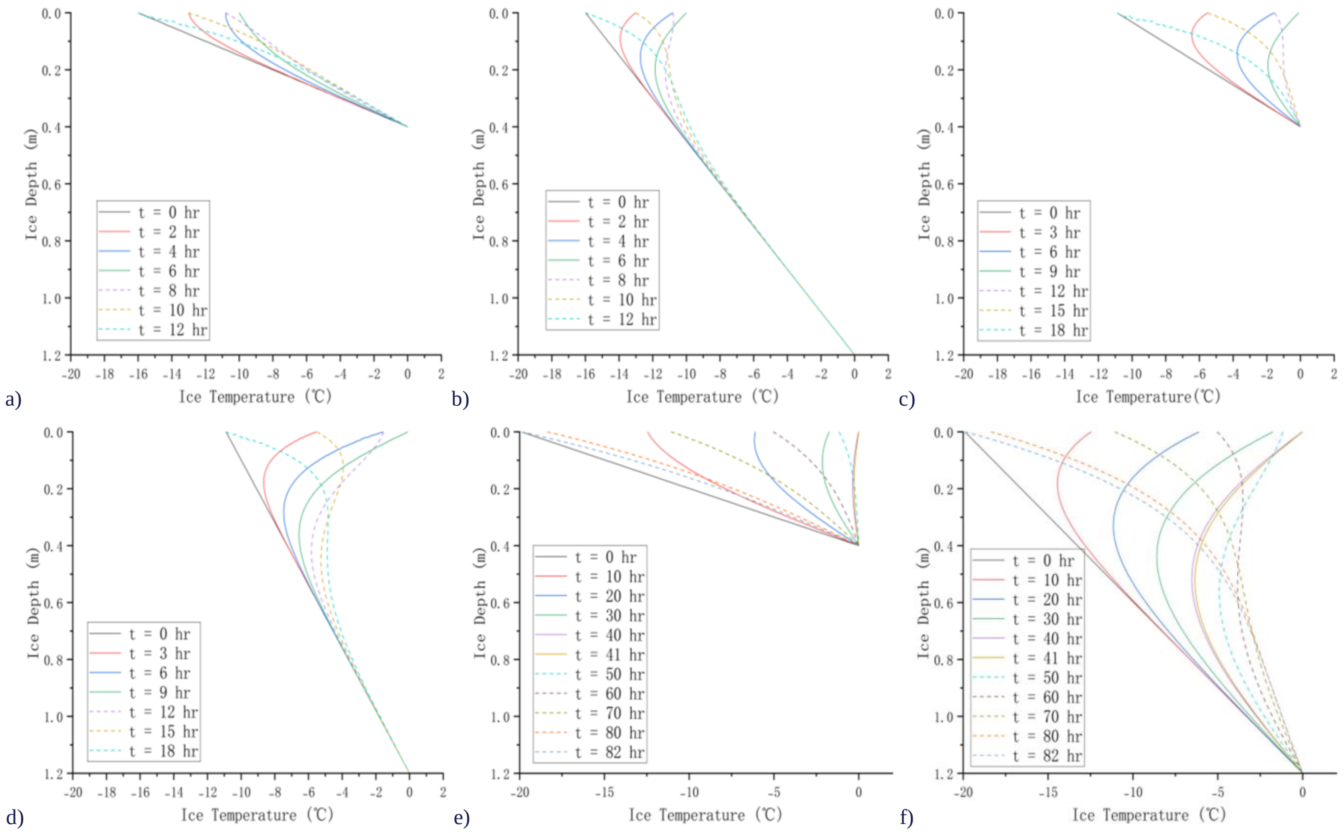

Fig. 5. Spatiotemporal variation of temperature inside the ice cover with ice depth: a), b), c), d), e), f) – operating mode (1), (2), (3), (4), (5), (6), respectively.

From Fig. 5, the temperature field at the initial moment (t = 0 h) varies linearly with the increase of ice depth, assuming that the heat transfer of ice cover is sufficient. Assuming that the surface temperature of ice cover changes with the temperature, while the lower surface of ice cover is affected by the water temperature and remains constant. The temperature field inside the ice cover changes nonlinearly.

When the thickness of ice cover is 0.4 m, there are different degrees of changes in the temperature field inside the ice cover in operating modes (1), (3), and (5). The longer the duration of temperature rise, the greater the amplitude of internal temperature field changes. In operating mode (5), when the temperature increases continuously for 41 h, the temperature field of the ice cover is roughly evenly distributed. In this case, the thermal expansion stress of the ice cover should be high. However, as the strength of ice decreases with increasing temperature, its stress field distribution is complex and will be analysed later.

When the thickness of the ice cover is 1.2 m, the temperature field inside the ice cover has different changes in operating modes (2), (4), and (6). When the temperature rises continuously for 6 h, the changes in the temperature field inside the ice cover are mainly concentrated in the upper 2/3 depth of the ice cover. The temperature change of the ice cover is not significant, around 1/3 of the thickness of the surface between the ice cover. As the duration of temperature increases, the range of temperature field changes inside the ice cover gradually expands. When the temperature rises continuously for 9 h, the temperature change range extends downward by about 20 K. When the temperature rises continuously for 41 h, the temperature field within the entire ice cover will change. When the surface of the ice cover begins to cool, the temperature inside the ice cover further increases, which will also affect the thermal expansion stress of the ice. This also explains the phenomenon that the maximum thermal expansion force generally does not occur on the surface of the ice cover where the temperature rises the most, but rather at a certain location inside the ice cover [14]. Based on the above analysis of temperature, when the temperature rises continuously for a long time and the thickness of the ice cover is small, the temperature field inside the ice cover changes significantly, with a wide range of impacts and drastic spatiotemporal changes, indirectly explaining the cause of ice damage to small-diameter piles at the end of November.

4. Conclusions

The temperature field of ice cover is influenced by multiple factors such as temperature and water temperature, and its changes are complex. Through one-dimensional heat conduction equation simulation, it is known that the propagation speed and amplitude attenuation of temperature waves inside the ice cover are frequency dependent. In practice, such as ice damage of a small diameter pile at the Daqing Lake wharf, the temperature field inside the ice cover changes nonlinearly during the heating process. Different thicknesses of ice cover (0.4 m and 1.2 m) and the duration of temperature rise have a significant impact on it. This characteristic is closely related to ice damage, where temperature rise leads to ice cover expansion, and uneven changes in the temperature field cause internal stress changes, which are important factors causing ice damage to small-diameter piles.

The simulation results show that when the surface of the ice cover cools, the internal temperature of the ice cover will still rise, which leads to the redistribution of thermal expansion stress of the ice. This discovery deepens the understanding of the mechanism of ice damage and provides a key theoretical basis for precise prevention and control of ice damage to small-diameter piles.

The results will help optimize the design and construction plans of small-diameter pile structures in cold regions, and improve their resistance to ice damage. Future research can explore the distribution of stress of ice cover, improve prediction models of ice damage, provide more comprehensive and accurate guidance for engineering practice, and promote the development of ice damage prevention and control technologies.

Acknowledgements

The work was supported by the Heilongjiang Province Philosophy and Social Sciences Research Planning Project 2023 (Research on the Evolutionary Game of Multi-Agent Collaborative Innovation in Intelligent Construction under the ‘Dual Carbon’ Goal, 23GLD043), Research Business Expenses for Provincial Research Institutes in 2024 (Research on the Calculation of Standard Frozen Depth of Seasonal Frozen Soil in Heilongjiang Province, CZKYF2024-1-B004) and Heilongjiang Province Postdoctoral General Grant Project 2023 (Research on the Mechanism and Prevention Technology of Pile Foundation Ice Damage in High Latitude Areas, LBH-Z23260).

References

[1] Huiban, F., Millan, R., Kjeldsen, K.K., Andresen, C.S., Dømgaard, M., Dehecq, A., Brunt, S., Khan, S.A., Mouginot, J., & Bjørk, A.A. (2024). Regional ice flow piracy following the collapse of Midgaard Glacier in Southeast Greenland. *Nature Communications*, 15(1), 1−10. doi: 10.1038/s41467-024-54045-z

[2] Urban, M.C. (2020). Life without ice. *Science*, 367(6479), 719−719. doi: 10.1126/science.abb2021

[3] Wei, P.C., Niu, W.W., Yao, C., He, Z.Y., Zheng, Y.Y., & Ma, W. (2024). Microscopic Thermo-Mechanical Properties and Phase Transition of Bulk Ice-Ih. *Numerical and Analytical Methods in Geomechanics*, 48(18), 4491−4505. doi: 10.1002/nag.3856

[4] Barker, A., Bruneau, S., & Colbourne, B. (2021). Bulk Adhesion of Ice to Concrete: Review of Test Programs. *Journal of Cold Regions Engineering*, 35(3), 03121001. doi: 10.1061/(ASCE)CR.1943-5495.0000253

[5] Staroszczyk, R. (2021). On Maximum Forces Exerted by Floating Ice on a Structure Due to Constrained Thermal Expansion of Ice. *Marine Structures*, 75, 102884. doi: 10.1016/j.marstruc.2020.102884

[6] Wang, E.L., Leng, Y.P., Han, H.W., Xiao, Y. & Fu, X. (2020). Indoor simulation test of ice temperature expansion force and analysis of related factors. *Hydro-Science and Engineering*, (3), 1−10. doi: 10.12170/20191009001

[7] Marchenko, A., Lishman, B., Wrangborg, D., & Thiel, T. (2016). Thermal Expansion Measurements in Fresh and Saline Ice Using Fiber Optic Strain Gauges and Multipoint Temperature Sensors

Based on Bragg Gratings. *Journal of Sensors*, 2016(1), 1−13. doi: 10.1155/2016/5678193
[8] Cox, G.F.N. (1984). A preliminary investigation of thermal ice pressures. *Cold Regions Science & Technology*, 9(3), 221−229. doi: 10.1016/0165-232X(84)90069-7
[9] Sharapov, D.A., & Andreeva. S.A. (2024). Features of the Calculation of Ice Load Due to Thermal Expansion. *Power Technology and Engineering*, 57(5), 697−704. doi: 10.1007/s10749-024-01721-1
[10] Liu, X.Z., Li, B., Zhang, Y.D. & Zhang, C. (2022). Comprehensive Fracture Model of Reservoir Ice Layers in the Northeastern Cold Region of China. *Sustainability*, 14(12), 7326. doi: 10.3390/su14127326
[11] Staroszczyk, R. (2018). Floating Ice Plate Failure Due to Its Thermal Expansion at the Surface. *Ocean Engineering*, 158, 331−337. doi: 10.1016/j.oceaneng.2018.03.072
[12] Han, H.M., Shen, L., Cao, M.S., Wei, L., & Qian, X.D. (2024). On the ice induced damage of reservoir drainage tower: A thermal stress-involved contact simulation. *Engineering Failure Analysis*, 160, 108203. doi: 10.1016/j.engfailanal.2024.108203
[13] Jiang, J.G., Li, X.T., Su, C.Z., Guo, X.J., He, M.Z.B. & Zeng, Y. (2023). Finite Element Analysis of the Influence of Ice Temperature Expansion Force on Surface Water Quality Monitoring System. *Vibroengineering Procedia*, 48, 107−112. doi: 10.21595/vp.2023.23140
[14] Li, J.X., Yang, J.J., Liu, Q., Xu, J., Zhang, W.Y., & Yang, Q.Y. (2024). Investigation of the temperature field of the ice sheet in a prefabricated curling ice rink: Experiment and finite element simulation. *Applied Thermal Engineering*, 251, 123636. doi: 10.1016/j.applthermaleng.2024. 123636
[15] Kolerski, T., Radan, P., & Gąsiorowski, D. (2021). Ice Load Characteristics on Floating Photovoltaic Platform. *Energies*, 14(9), 2466. doi: 10.3390/en14092466
[16] Beltrami, H. (2001). On the relationship between ground temperature histories and meteorological records: A report on the Pomquet station. *Global and Planetary Change*, 29(3−4), 327−348. doi: 10.1016/S0921-8181(01)00098-4
[17] Leppäranta, M. (2015). *Freezing of Lakes and the Evolution of their Ice Cover*. Springer Berlin Heidelberg (1st ed.). doi: 10.1007/978-3-642-29081-7
[18] Sanderson, T.J.O. (1978). Thermal Stresses near the Surface of a Glacier. *Journal of Glaciology*, 20(83), 257−283. doi: 10.3189/S0022143000013836
[19] Zhang, H., Bian, J.M., & Wan, H.L. (2021). Hydrochemical appraisal of groundwater quality and pollution source analysis of oil field area: A case study in Daqing City, China. *Environmental Science and Pollution Research*, 28(15), 18667−18685. doi: 10.1007/s11356-020-12059-2
[20] Tanary, S., Fahim, A., & Munro, M. (1994). Hydrostatic Pressure Loading due to Ice Formation in Manholes. *Journal of Cold Regions Engineering*, 8(4), 121−132. doi: 10.1061/(ASCE)0887-381X(1994)8:4(121)